

Log-Based Physical Properties of the CRP-1 Core, Ross Sea, Antarctica

F. NIESSEN¹, R. D. JARRARD² & C. BÜCKER³

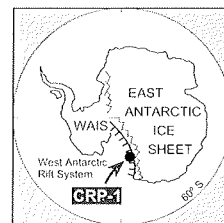
¹Alfred Wegener Institute for Polar and Marine Research, P.O. Box 120161, D-27515 Bremerhaven - Germany

²Dept. of Geology and Geophysics, University of Utah, 135 S 1460 East, Rm. 719,
Salt Lake City UT 84112-0111 - USA

³Federal Institute for Geosciences and Natural Resources, Stilleweg 2, D-30655 Hannover - Germany

Received 20 July 1998; accepted in revised form 15 October 1998

Abstract - P-wave velocity, wet bulk density, and magnetic susceptibility are measured on the whole CRP-1 core to analyse their down-core patterns and relationships with lithology, and to interpret the compaction and exhumation history. Velocity and density-based porosity are inversely correlated and strongly dependent on compaction and lithology. Fractional porosities of sands, silts and muds exhibit a nearly linear compaction trend from 0.5 to about 0.2 between 20 and 120 metres below sea floor (mbsf). This anomalously steep gradient suggests that overconsolidation of the lower portion is more important than the effects of lithology. Correction of porosities for both grain-size effects and the compaction trend implies overconsolidation even for some non-diamict units, probably related to glacial loading during deposition of overlying basal tills. Exhumation of the Miocene section, now unconformably overlain by Quaternary sediments above 43.15 mbsf, is estimated to be between 200 and 700 m based on different compaction trends. The down-core trend of magnetic susceptibility is largely independent of compaction and lithology. A relatively abrupt up-core increase in magnetic susceptibility from about 200 to more than 2 000 (10^{-6} SI) occurs at 63.2 mbsf, probably related to the onset of volcanic activity of McMurdo Volcanic Province at 19 Ma. Magnetic susceptibility below 63.2 mbsf is cyclic on a scale of tens of metres and correlates with the sequence stratigraphy of CRP-1. High frequency oscillations of magnetic susceptibility appear mostly as distinct spikes rather than cycles. The only exception is susceptibility cycles in the lowermost mudstone unit, where Milankovitch forcing is possible but remains questionable. A cluster analysis log calculated from physical properties does not match lithological unit and sequence boundaries, which indicates as-yet-unidentified petrophysical variations at CRP-1.



INTRODUCTION

The Cape Roberts Project (CRP) was initiated for two main reasons: (i) to discover if there were ice sheets on Antarctica causing fluctuations in world-wide sea levels before the glaciations of the last 36 million years, and (ii) to date the rifting of the Antarctic continent in order to help understand the formation of the Transantarctic Mountains and the Ross Sea. The first drilling location, CRP-1, lies in 150 m of water, 16 km from Cape Roberts (Victoria Land), which is about 125 km north-northwest of McMurdo Station. Quaternary and Miocene strata of the Victoria Land Basin were cored to a total depth of about 148 metres below sea floor (mbsf). The age of the Miocene sediments is about 17 to 24 Ma, much younger than expected from pre-drilling interpretation of the seismic stratigraphy (Cape Roberts Science Team, 1998). A major unconformity, with a hiatus of about 15 m.y., marks the Quaternary/Miocene boundary at 43.15 mbsf.

In the drillsite laboratory, whole-core physical properties logs were obtained for magnetic susceptibility, P-wave velocity and density/porosity, at depth intervals of 2 cm. As previously discussed in the Initial Report (Cape Roberts Science Team, 1998), not all unit boundaries seen in the lithological logs are also defined in the physical

properties. Therefore, initially six physical property units were defined and described based on both amplitudes and degree of scatter in the data sets. The latter was interpreted to be controlled by the content of lonestones because, in general, physical properties in diamicts show larger scatter than in other units. Some variations in the physical properties could not be linked to lithological boundaries and remained obscure.

The clear advantage of log-based whole-core physical properties is their high vertical resolution of 2 cm, which can be obtained if the core is complete and undisturbed, providing the highest stratigraphic resolution currently available for the CRP-1 core. The disadvantage is that the interpretation of physical properties is often difficult if they stand alone, because first-order environmental control is often hard to distinguish from second-order diagenetic overprint. The tremendous amount of CRP-1 data, which have been produced by various disciplines (Cape Roberts Science Team, 1998, this volume), offer a good opportunity to better understand the physical property results by comparing them with other results, such as lithology, sequence stratigraphy, grain size and lonestone abundance, as is addressed in this paper. Here, we examine the downcore trends and patterns in the physical property logs of the CRP-1 core. The relationship of whole-core porosity and

velocity and the comparison of whole-core and plug-sample physical properties are discussed elsewhere (Niessen & Jarrard, this volume; Brink & Jarrard, this volume).

Porosity and P-wave velocity of CRP-1 sediments are affected by both depositional conditions and post-depositional alteration such as compaction, fracturing and diagenesis. Porosities of most siliciclastic sediments depend on grain size and compaction history (Hamilton, 1976). Analyses of very shallow (mostly <10 mbsf) marine sediment core samples show that initial porosity depends strongly on average grain size and sorting: well-sorted sands have porosities of only about 40%, whereas clays have porosities of up to 80% (e.g., Shumway, 1960a, 1960b; Hamilton, 1976). Initial porosities are subsequently decreased by both mechanical compaction and chemical diagenesis. If compaction trends can be identified for different lithologies and corrected for primary grain-size effects, one can identify porosity anomalies, such as those generated by glacial overconsolidation. This is of particular interest for the CRP-1 site which may have been frequently overridden by glaciers.

The main carrier of magnetisation of the CRP-1 sediments is probably multi-domain magnetite (Cape Roberts Science Team, 1998). Magnetite has a significantly higher susceptibility ($k = +10^{-2}$) than most common minerals (-10^{-6} to $+10^{-6}$) and is usually more abundant in volcanic rocks and ashes (e.g., Thompson & Oldfield, 1986) than in most sediments. Volcanically derived debris is common in the CRP-1 section, including both large clasts (lonestones) derived from the volcanic Ferrar Group in the Transantarctic Mountains (Kyle, this volume) and sand-sized volcanic glass and lava, largely related to the Erebus/McMurdo Volcanic Province of Ross Sea (Cape Roberts Science Team, 1998). We can therefore expect that input of material from these different provenances would leave imprints on the magnetic susceptibility record. Moreover, the vertical resolution should enable us to identify any cyclicities present in the record. Susceptibility oscillations in marine sediments often have been demonstrated to be controlled by Milankovitch forcing (e.g., Bloemendal & de Menocal, 1989; Shackleton et al., 1995; Mienert & Chi, 1995).

Combining different physical properties such as density, velocity and magnetic susceptibility by cluster analysis allows identification of so-called electrofacies, core units with distinct combinations of core properties (e.g., Serra, 1986). Here we will demonstrate that cluster analysis of the core-physical properties is a useful and objective method for identifying distinctive downcore variations in addition to the readily visible lithologic units.

METHODS

During the CRP-1 coring campaign, the drillsite laboratory work included non-destructive, near-continuous determinations of wet bulk density (WBD), P-wave velocity (V_p), and magnetic susceptibility at 2-cm intervals. The Multi Sensor Core Logger (MSCL, Geotek Ltd., UK) was used to measure core temperature, core diameter, P-wave

travel time, gamma-ray attenuation and magnetic susceptibility. The technical specifications of the MSCL system are summarised in the CRP-1 Initial Report (Cape Roberts Science Team 1998). The MSCL system can log cores with a measuring velocity of about 3 m/h. The cores were logged in plastic carriers (Fig. 1) to avoid destruction of non-consolidated rock material. Core carriers were confirmed to be non-magnetic. The orientation of the P-wave and gamma-ray sensors was horizontal.

Magnetic susceptibility was measured in SI-mode using a Bartington MS-2 metre and a loop sensor of 80 mm internal diameter. Because the geometry of the loop sensor does not allow a direct determination of volume susceptibility, we compared CRP-1 volume susceptibility determined in discrete samples (Roberts et al., this volume) to susceptibility measured with the Bartington at the same depth (Fig. 2). The resulting linear regression was used to convert loop susceptibility to volume susceptibility (Vol Sus 10^{-6} SI):

$$\text{Vol Sus} = 14.984 * \text{Loop Sus} - 5.7053, (R=0.924)$$

where Loop Sus is the Bartington metre reading (10^{-5} SI) corrected for core diameter and loop diameter as described in detail elsewhere (Cape Roberts Science Team, 1998).

P-wave pulses for whole-core measurements had a frequency of 500 kHz. The methodology of plug velocity measurements is described by Brink & Jarrard (this volume). Whole-core P-wave velocities were calculated from the core diameter and travel time after subtraction of the P-wave travel time offset including travel time through the transducer caps plus electronic delay (Cape Roberts

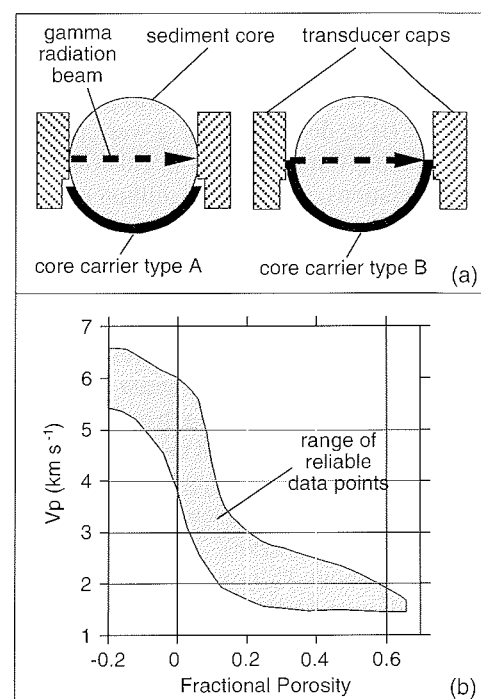


Fig. 1 - a) Cross section of P-wave transducer caps and core carriers used during the CRP-1 field campaign. The gamma radiation beam focused through the centre of the core. b) Range of reliable data points (envelope drawn after Niessen & Jarrard, this volume). Data outside the shaded area were removed from the files.

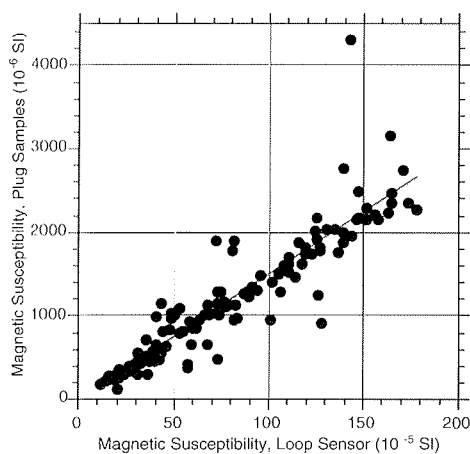


Fig. 2 - Comparison of whole-core magnetic susceptibility (Bartington loop sensor, 10^{-5} SI) to volume magnetic susceptibility determined in plug samples from CRP-1 (Cape Roberts Science Team, 1998).

Science Team, 1998). This offset was determined by bringing both transducer caps in direct contact. P-wave velocities are normalised to 20°C using the temperature logs. Core temperature was measured by a calibrated infra-red sensor. For most of the core sections we have used core carriers and transducer caps designed to allow a direct contact of both transducers with the core surface (carriers type A, Fig. 1). However, some core sections were insufficiently lithified and did not allow direct transducer contact. In such cases half-liner (carriers type B, Fig. 1) were used in order to keep the cores in proper shape. Unfortunately, carriers of type B did not allow proper sound transmission, which led to major gaps in the P-wave data set between about 45 and 93 mbsf.

Wet bulk density (WBD) was determined from attenuation of a gamma-ray beam transmitted from a radioactive source (^{137}Cs). The beam of 5 mm in diameter was focused through the core above the core carrier in case of use of carriers type A (Fig. 1). Using carriers type B some gamma attenuation by the half liners could not be avoided. For each three-metre piece of core 20 values of attenuation through air were measured to ensure detector drift was monitored at least twice per day. The mean counts of these air measurements were then used to calculate the natural logarithm of the ratio of attenuated (core) over non-attenuated (air) gamma counts per second so that long-term drift of the detector did not affect WBD. For type B carriers, non-attenuated gamma counts were measured with an empty half-liner on the rail to eliminate the effect of attenuation by the half liner on core WBD. In case of use of carriers B a constant core diameter of 61.1 mm was assumed, because a core thickness determination was not possible if the P-wave transducers were not in direct contact with the core. The gamma detector was calibrated once at the beginning of CRP-1 coring activity, using aluminum, carbon and nylon of known densities. This calibration included the elimination of errors related to variable count rates (Weber et al., 1997) such as caused by detector drift. The counting time was 10 s per depth interval. WBD was calculated from the ratio of attenuated (core) over non-attenuated (air or half-liner)

gamma counts (Weber et al., 1997), considering the core diameter and specific gamma attenuation coefficients of water and rock; the calculation is described in more detail in Cape Roberts Science Team (1998). Porosity is computed from the WBD assuming a constant grain density of 2.7 Mg m^{-3} and pore-water density of 1.02 Mg m^{-3} .

The grain density of 2.7 Mg m^{-3} used in this paper is based on CRP-1 core-plug analyses of Brink & Jarrard (this volume). Porosities presented here differ from those previously calculated from the same WBD record and shown in the Initial Report (Cape Roberts Science Team, 1998) because of revised grain density. In order to avoid generating negative porosities, calculations in the Initial Report assumed a grain density of 2.97 Mg m^{-3} , not 2.65 Mg m^{-3} as stated by Cape Roberts Science Team (1998).

Downcore logs of WBD and porosity comprise nearly complete datasets for all lithological units. Only for those depth intervals where major disturbances were observed (gaps or heavily crumbled core) were data eliminated, based on core images. For the rest of the P-wave and WBD/porosity data, we defined an envelope in a V_p versus porosity cross-plot (Niessen & Jarrard, this volume) in order to further identify and eliminate unreliable data points (Fig. 1b).

Velocity can be predicted from porosity. In order to perform a cluster analysis using V_p , WBD and magnetic susceptibility, a complete data set of all parameters is needed. Therefore the existing gaps in the velocity record (Fig. 3) were filled using a second-order polynomial fit to data in the velocity range from 1.8 to 4.5 km s^{-1} (Niessen & Jarrard, this volume; Bückner et al., this volume):

$$V_p = 13.4907 - 12.379 * \text{WBD} + 3.1948 * \text{WBD}^2 \\ (R=0.97)$$

Thereafter, WBD, V_p and susceptibility records were resampled for 10 cm depth intervals to ensure linear depth spacing between data points. For the multivariate cluster analysis, the PC-based software package WINSTAT 3.1 was used. A complete linkage, hierarchical cluster analysis (using a Euclidean norm, "Ward-method") (Davis, 1973) was performed on the core physical property data WBD, V_p and susceptibility.

RESULTS AND DISCUSSION

OVERVIEW OF DENSITY AND POROSITY VARIATIONS

CRP-1 densities determined by gamma ray absorption on whole-core sections (this paper) were compared with those from plug samples by Brink & Jarrard (this volume). The two data-sets are consistent. Downcore trends of whole-core WBD and porosity are exact mirror images because porosity is calculated from WBD (see above). Therefore, our compaction analyses are confined to porosity, which is the major control on WBD in marine sediments (e.g., Hamilton, 1976).

The down-core trends of P-wave velocity and porosity of CRP-1 (Fig. 3) show five characteristic features: (i) in

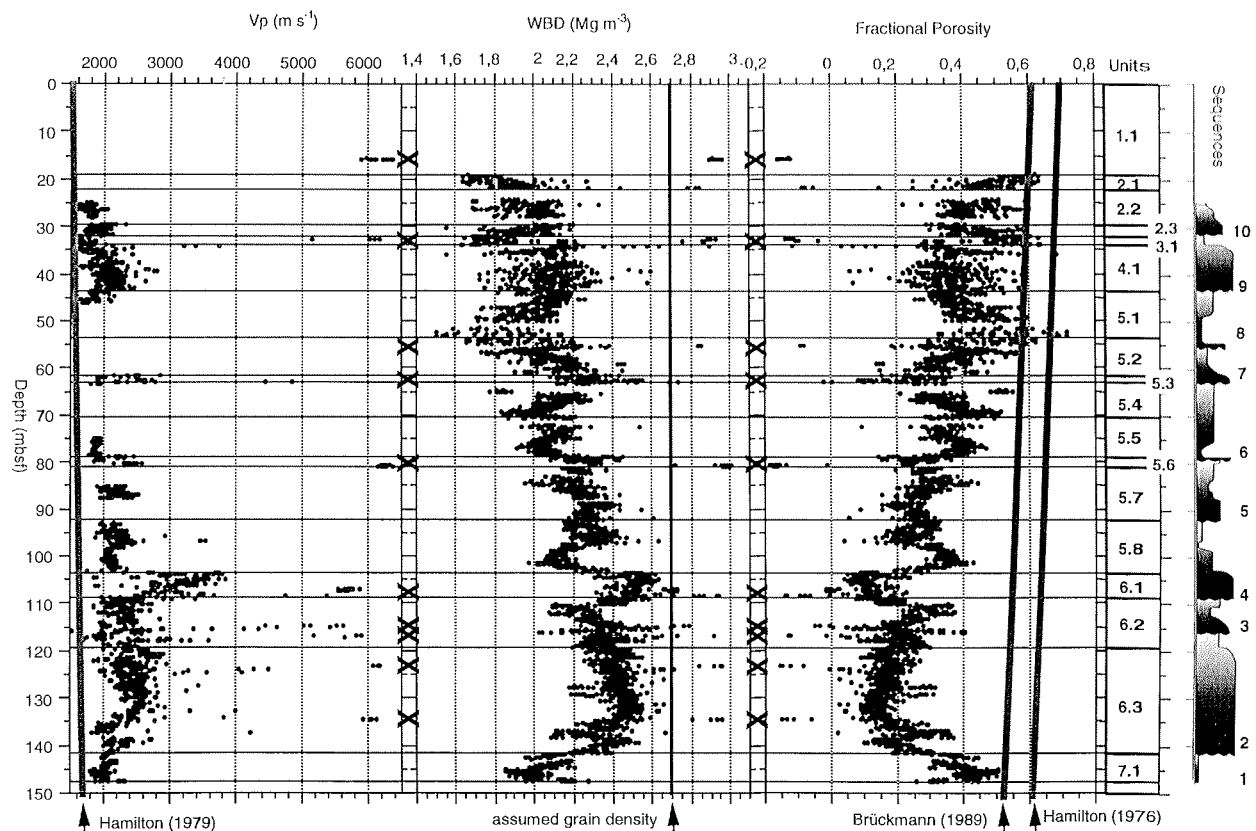


Fig. 3 - Whole-core logs of P-wave velocity (V_p), Wet Bulk Density (WBD), and fractional porosity of CRP-1, compared to lithological units and sequences (both from Cape Roberts Science Team, 1998) and typical down-core trends published by Hamilton (1976, 1979) and Brückmann (1989). Bold line on WBD plot is grain density assumed for conversion of WBD to porosity. X is depth location of large clast from the 4-m lithology logs (Cape Roberts Science Team, 1998).

general, porosity and velocity are inversely correlated, (ii) no distinct change marks the unconformity between the Quaternary and Miocene at 43.15 mbsf, (iii) the Miocene section is characterised by steep down-core gradients, in particular for porosities which decrease from about 0.55 in Unit 5.1 to less than 0.2 in Unit 6.3, (iv) both velocity and porosity have local variations (about 0.1 to 0.2 in fractional porosity) superimposed on this down-core trend, and (v) a few isolated layers have very high velocities and porosities that are very low (or even apparently negative) (marked with an "X" in Fig. 3). Each of these patterns is considered in more detail below.

(i) The relationship between porosity and velocity is discussed in detail in a separate paper (Niessen & Jarrard, this volume). Velocity can be described by a second or third order polynomial function of porosity. The down-core velocity gradient is less steep than would be predicted from applying empirical velocity-porosity relationships to the porosity gradient, resulting in relatively low velocities at porosities between 0.1 and 0.4. However, nearly all P-wave velocities are higher than expected based on typical depth gradients for unconsolidated marine sediments (Hamilton, 1976). The strongest positive deviations from the Hamilton trend are seen in Units 6.1 and 6.3 (Fig. 3).

(ii) The fact that no step decrease in porosity is evident at the 43.15 mbsf unconformity between Quaternary and Miocene sediments, despite probable major differences in burial history, may be partly explained by the transition from smectite-rich uppermost Miocene to smectite-poor

Quaternary sediments (Ehrmann, this volume). This may introduce an undetected matrix density change that could obscure a subtle porosity offset. We cannot exclude, however, that some core data are affected by lack of lithification or drilling artifacts which caused alteration after recovery as discussed in Cape Roberts Science Team (1998). In particular the top of the Miocene section is affected by bad recovery. In addition to possible changes in matrix density, noisy data might obscure any change in porosity.

(iii) The compaction-induced downhole reduction of fractional porosity (and corresponding increase in velocity) is much steeper than is typically observed at these burial depths. Nearly all CRP-1 porosities lie well below reference trends of *in situ* porosities, both for unconsolidated terrigenous sediments (Fig. 3) (Hamilton, 1976) and for silty clays and sands (Brückmann, 1989). The only exception is the lower part of Unit 5.1, where porosities of more than 70% were determined in unconsolidated sands. This is probably a drilling artifact, caused by injection of drilling fluid and mud (Cape Roberts Science Team, 1998). The strongest shifts away from the normal compaction trend of sand and silty clay are observed in Units 6.1 and 6.3 (Fig. 3).

(iv) Based on porosity alone, three major lithologic categories are distinguished: sand/silt/muds, diamicts, and claystones. Downcore lithologic changes induce associated local variations in porosity and velocity. Most diamicts, in particular those in Units 5.3, 5.6, and 6.1, are

characterised by significantly lower porosity and higher velocity than other lithologies. Diamicts are very poorly sorted, so their porosities may be expected to be slightly lower than those of sands and silts. In contrast, clays usually have higher initial porosities than any other siliciclastic sediment (Hamilton, 1976), and this difference is retained for the claystones at the bottom of CRP-1: their porosities of about 0.5 are 0.2 higher than is extrapolated from the compaction trend of overlying sediments. The claystone porosities are also about 0.1 higher than those of the muds, which are much more poorly sorted and consequently lower in porosity than clays.

(v) Very high velocities and apparently negative porosities are mostly observed in depth intervals where the entire core consists of a single large lonestone (Niessen & Jarrard, this volume). Many lonestones, and particularly mafic ones, have grain densities higher than the 2.7 Mg m^{-3} value obtained for CRP-1 sediments, resulting in negative apparent porosities. Details of the depth location and physical properties of these isolated large lonestones are given in Niessen & Jarrard (this volume).

COMPACTION, OVERCONSOLIDATION, AND EXHUMATION

Pressure increase associated with burial accomplishes a modest degree of mechanical compaction for sands. The number and type of grain contacts change initially by more compact arrangement and later, with deeper burial, by plastic deformation of weaker minerals (Taylor, 1950; Hayes, 1979). Mechanical compaction is more intense in shaly sediments, as the initial "cardhouse" fabric of randomly oriented clay particles is forced into a generally parallel arrangement (*e.g.*, Hedberg, 1936; Magara, 1980). With greater burial, chemical diagenesis (including pressure solution, recrystallisation, and replacement) replaces physical compaction as the dominant mechanism of porosity reduction (*e.g.*, Hayes, 1979; Foscolos, 1990; Hutcheon, 1990).

Is there a simple way to examine the compaction history of the CRP-1 site? The CRP-1 sandstones, siltstones, and mudstones lie along a simple, linear compaction trend (Fig. 4a). That this is true is surprising, as both the initial porosities (Shumway, 1960a, 1960b; Hamilton, 1976) and compaction trends (Hamilton, 1976; Brückmann, 1989) of these three lithologies are usually quite different. In comparison, CRP-1 diamicts have porosities that are similar to, or significantly less than, the sand/silt/mud trend (Fig. 4b). Diamictites for the upper portion of Unit 6.3 (119-135 mbsf) exhibit very low porosity dispersion and average values that fit the sand/silt/mud trend remarkably closely. In contrast, the porosities for Units 5.3 (61.5-63.2 mbsf) and 6.1 (103.4-108.8 mbsf) are anomalously low (Fig. 4b). Lonestone volume does not significantly decrease porosity, except for very large lonestones (Niessen & Jarrard, this volume).

Thus, an additional compaction mechanism may be indicated: overconsolidation associated with glacial loading during deposition of basal tills. For example, basal tills in Prydz Bay have porosities about 0.12 lower than proximal glacial marine tills (Ollier & Mathis, 1991). Lonestones for

Units 5.3 and 6.1 appear to exhibit preferred orientation fabrics characteristic of basal tills, but only the Unit 5.3 fabric is statistically significant at the 95% confidence level (Cape Roberts Science Team, 1998). In addition, analysis of fractures of the CRP-1 core indicates a vertical maximum compressive stress during deformation for both Miocene and Quaternary units. Such stress is characteristic of continental rift regimes but may also have been caused by ice load (Cape Roberts Science Team, 1998; Passchier *et al.*, this volume). If significant ice loading has occurred, overconsolidation may not have been restricted to diamicts but may have also affected some of the sand, silt and mud underlying the diamicts. Possibly, this could explain the enormously steep compaction trend for sands, silts, and muds.

What evidence would indicate overconsolidation in non-diamict units? The relatively high porosity of 0.5 in the claystone at the bottom of CRP-1 core demonstrates that clay content is an important control for porosities superimposed on compaction. The compaction trend of sand, silt and mud units (Fig. 4a) can be described by a simple linear regression:

$$f = 0.5574 - 0.002914 * Z \quad (R = 0.75)$$

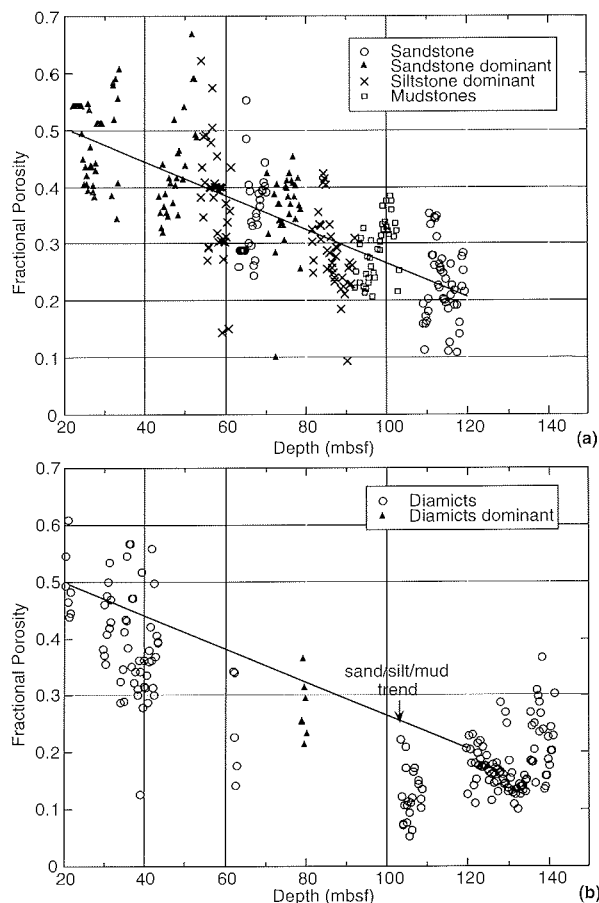


Fig. 4 - a) Porosity as a function of depth in sandstone, sandstone dominant, siltstone dominant, and mudstone units of CRP-1. Also shown is the compaction trend based on linear regression of these data. b) Porosity as a function of depth in diamict and diamict dominant units of CRP-1. Both plots (4a & b) are based on a porosity log resampled at 10-cm depth intervals from whole-core data.

where f is fractional porosity and Z is depth (mbsf). Niessen & Jarrard (this volume) removed this linear compaction trend from porosities, resulting in porosity residuals (defined as the difference between observed porosity and that predicted from depth). Residual porosities were then compared to measured clay contents (Ehrmann, this volume). Statistically, the influence of clay content on the porosity residual can be described by a simple linear regression (Niessen & Jarrard, this volume):

$$f_{\text{res}} = -0.06946 + 0.0097413 * c \quad (R = 0.6)$$

where f_{res} is the residual of fractional porosities and c is the clay content in weight % <2 μm . We have used this regression to remove the effect of clay content on fractional porosity. Although grain-size data are sparse, some depth intervals clearly have fractional porosities about 0.1 less than expectations, based on their clay content and overall compaction trend (Fig. 5). Thus, overconsolidation is implied even for some units that are not diamicts. This is particularly true for the depth interval from 60 to 110 mbsf, where 34 out of 45 samples suggest overconsolidation (Fig. 5). We conclude that glacial loading has overcompacted both diamicts and other sediments at some point in the history of CRP-1. This accounts for the anomalously steep sand-silt-mud compaction trend in figure 4a. Overcompaction generates so much porosity variation within CRP-1 that the influence of clay content on porosity (Figs. 4a & 5) is, by comparison, a relatively subtle second-order effect. Its influence on this trend means, however, that the actual compaction trend is gentler and the amount of real overcompaction for 60 to 110 mbsf is even larger than indicated in figure 5. If a grain-size correction is applied, the Quaternary sediments of CRP-1 do not exhibit a clear trend toward negative fractional porosity residuals (Fig. 5) which suggests that there is no, or at least no clear indication of, overcompaction above the unconformity at 43.15 mbsf.

Seismic profiles across the CRP-1 site demonstrate that some exhumation has occurred prior to the deposition of the Quaternary (Cape Roberts Science Team, 1998). Despite the extreme overconsolidation, can one estimate how much burial and exhumation the Miocene section has experienced? Porosity/depth or velocity/depth patterns can be used to estimate amount of exhumation at a well, if a reference porosity/depth or velocity/depth trend is available for similar formations in a nearby region with no exhumation. However, no uneroded reference well is available for CRP-1. Heasler & Kharitonova (1996) proposed a method for estimating exhumation from a velocity/depth pattern without using a reference well, but Jarrard et al. (pers. comm.) found that this method is not robust. Shales, which have an exponential porosity/depth trend, provide the most reliable exhumation estimates (Magara, 1980). Unfortunately, the compaction trends of clays are so variable globally that the single claystone interval at CRP-1 provides an imprecise exhumation estimate of 0-600 m.

Figure 6 compares the fractional porosities from CRP-1 with typical compaction trends observed in sand and silty clay (Brückmann, 1989) and with the compaction trend

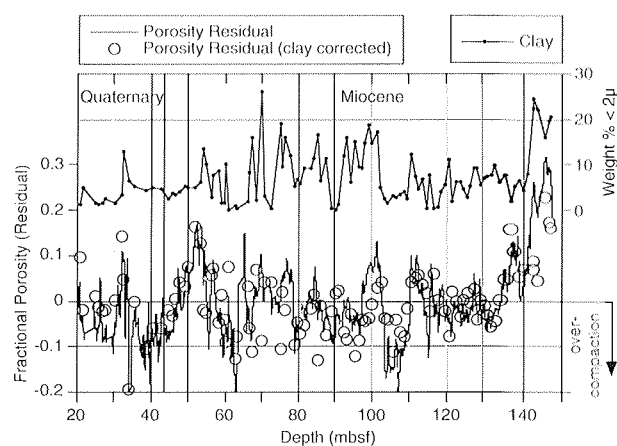


Fig. 5 - Fractional porosity residual and clay content (weight % <2 μm) as a function of depth in CRP-1. For the definitions of fractional porosity residual and fractional porosity residual (clay corrected), see text.

observed in the nearby CIROS-1 site. *In situ* densities measured in the CIROS-1 borehole (White, 1989) were converted to fractional porosity using a constant grain density of 2.67 Mg m^{-3} (Bücker et al., this volume). We placed the top of the CIROS-1 porosity gradient, which is based on data from non-diamict units, at a depth of 800 mbsf because the exhumation at the CIROS-1 site is estimated to be between 800 and 1 000 mbsf (e.g., Bücker et al., this volume). The gradient is highly compatible with the trends for sand and silty clay by Brückmann (1989). This suggests both that an estimated exhumation of about 800 m of the CIROS-1 site is reasonable, and that there is no apparent overconsolidation trend in the non-diamict units at the CIROS-1 site. If we assume that the relatively high fractional porosities of about 0.55 at the top of the Miocene of CRP-1 are real and not overconsolidated, the top of the CRP-1 compaction gradient can be placed at a depth of about 200 mbsf, suggesting that the site has experienced an exhumation of about 200 m. However, if one uses the average porosities of CRP-1 units to calculate a porosity gradient that ignores possible overconsolidation of Units 5.1, 5.2 and 7.1, then this gradient would be very similar to that of the CIROS-1 site if placed at a depth of 700 mbsf (Fig. 6). We estimate that the exhumation of the

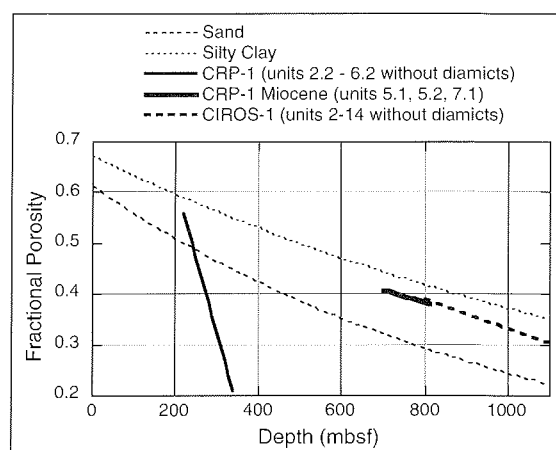


Fig. 6 - Comparison of different compaction trends. Sand and Silty Clay are from Brückmann (1989), CRP-1 is from this study, and CIROS-1 is calculated from data of White (1989).

CRP-1 site is between these two extremes. Figure 6 also demonstrates very well how anomalously overconsolidated those units are from which the sand-silt-mud consolidation trend of figure 4a was calculated.

DOWN-CORE LOGS OF MAGNETIC SUSCEPTIBILITY - LITHOLOGY AND SEQUENCES

The fact that the CRP-1 core exhibits a very strong gradient in porosity raises the question of whether the decrease of fractional porosities from about 0.7 to 0.1 has a significant influence on whole-core magnetic susceptibility. Only the contribution from mineral grains is relevant for whole-core magnetic susceptibility, because magnetic susceptibility of water is nearly zero ($-0.9 \cdot 10^{-6}$ SI). Therefore in high porosity layers, the magnetic susceptibility carried by the minerals would be underestimated because the pore volume filled with water "dilutes" the amount of magnetic carrier minerals in the core. We quantified this effect by assuming zero susceptibility for the pore volume:

$$K_p = K/(1-f)$$

where K is the measured magnetic susceptibility, corrected for core- and loop-diameter, and converted to volume susceptibility (10^{-6} SI), K_p is magnetic susceptibility (K) from which the effect of porosity is removed and f is fractional porosity (5-pt running average of the whole-core porosities of Fig. 3). The comparison of K and K_p (Fig. 7) demonstrates that the porosity effect is notable. Correction for porosity results in higher magnetic susceptibility amplitudes, in particular above 60 mbsf and

between 90 and 100 mbsf where porosity is increased because of lower compaction and/or increased clay fraction (Figs. 3 & 5). However a reversal of the downcore trend of magnetic susceptibility is not observed after correcting for porosity (Fig. 7). Therefore, we prefer to use the uncorrected susceptibility record for further interpretations because it has a higher resolution. Porosity correction leads to gaps in the dataset because porosity data are missing at fractured or crumbled core sections.

The downcore trend of whole-core magnetic susceptibility in CRP-1 (Fig. 7) shows three characteristic features: (i) a few isolated layers have either very high or very low magnetic susceptibilities, (ii) magnetic susceptibility below 63.2 mbsf appears to be cyclic on a scale of tens of metres, although some of the oscillations seem to be cut or incomplete, and (iii) relatively abrupt up-core increases in magnetic susceptibility occur at 63.2 and 31.89 mbsf, associated with increased dispersion. These increases would become even larger if the data were corrected for porosity (Fig. 7).

(i) Isolated layers with either extremely low or high magnetic susceptibility correlate with very high velocities and densities (Fig. 3). Niessen & Jarrard (this volume) showed that these measurements were located in depth intervals where the entire core consists of a very large lonestone. Those lonestones which exhibit very high magnetic susceptibility ($>5 \cdot 10^4 \cdot 10^{-6}$ SI) and velocity ($>6 \text{ km s}^{-1}$) are derived from dolerites of the Ferrar Group (Kyle, this volume); those with a velocity between 5 and 6 km s^{-1} and very low magnetic susceptibility are derived from granites (Niessen & Jarrard, this volume). This demonstrates that magnetic susceptibility on its own is not capable of indicating large lonestones except for the few

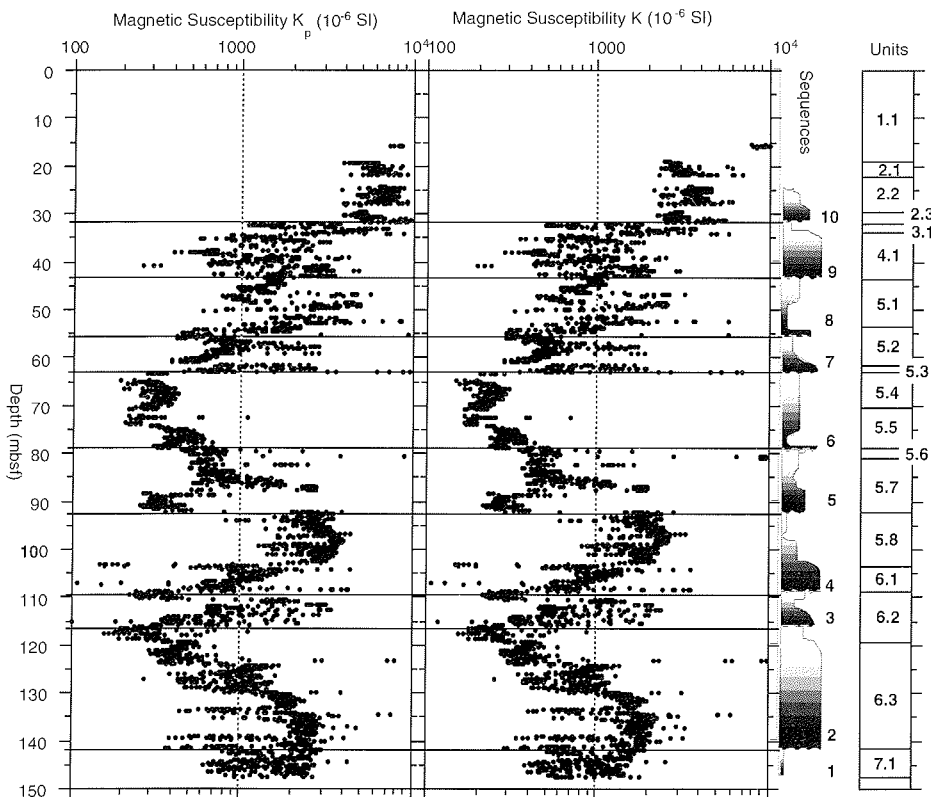


Fig. 7 - Whole-core magnetic susceptibility (converted to volume susceptibility) as a function of depth in CRP-1, compared to sequences and units (both from Cape Roberts Science Team, 1998). K_p refers to susceptibility which is corrected for porosity and K is based on measurements of the porous core.

dolerite clasts of the Ferrar Group. We tested this by comparing magnetic susceptibility with lonestone volume (Brink et al. this volume), excluding the largest lonestones by confining the analysis to intervals where lonestone volume is <25%. There is no correlation ($R=0.002$). Also, it is obvious that units without lonestones exhibit the same range in magnetic susceptibilities as units with significant lonestone volume such as diamicts. We conclude that the downcore variation of magnetic susceptibility cannot be interpreted in terms of lonestone volume in general. On the other hand, isolated lonestones which are derived from the Ferrar Group (dolerites) should cause small-scale isolated spikes in the downcore records, and many such spikes are evident in figure 7. A detailed analysis addressing this question has not been carried out yet.

(ii) Do the oscillations below 63.2 mbsf in the whole-core magnetic susceptibility record correlate with CRP-1 stratigraphy? Figure 7 compares the susceptibility pattern to lithological units and sequences identified in the core (Cape Roberts Science Team, 1998). Susceptibility gradients are evident within most lithologic units, and these gradients are often more distinctive than steps in magnetic susceptibility at unit boundaries. Also, the susceptibility pattern seems to be independent of lithology: diamict units (2.1, 2.3, 4.1, 5.3, 5.6, 6.1 and 6.3) are not distinctively different from units dominated by sandstone (2.2, 3.1, 5.1, 5.4, 5.5, 6.2), siltstone (5.2, 5.7), mudstone (5.8), and claystone (7.1) (Fig. 7). This observation is consistent with previously discussed evidence that magnetic susceptibility does not depend on lonestone volume.

In contrast to their weak dependence on lithology, cycles in physical properties generally do correlate with sequence stratigraphy (Cape Roberts Science Team, 1998; Fielding & Woolfe, this volume) (Fig. 7). Sequence boundaries are often characterised by steep gradients or shifts in magnetic susceptibility, certainly more often than unit boundaries. The sequence stratigraphy of CRP-1 is partly based on the premise that changes in grain size reflect changes in depositional energy and hence relative water level (Cape Roberts Science Team, 1998; Fielding & Woolfe, this volume). The presence of several cycles within the Miocene, defined by fining upward trends at the top of almost all diamict units, suggests a condensed succession representing several discrete intervals. Each of these intervals probably is bounded by a major hiatus because, in a relatively ice-proximal location like Cape Roberts, deposits recording progradation and advance are likely to be removed by erosion (Cape Roberts Science Team, 1998; Fielding & Woolfe, this volume). These hypothesised erosional events appear to be marked by major shifts in magnetic susceptibility, in particular at the boundary from sequence 3 to 4, 4 to 5 and 6 to 7 (Fig. 7). Unconformities may also explain why the cyclicity in magnetic susceptibility appears to be incomplete or cut.

Because CRP-1 sequences are mostly defined by fining upward trends, the question arises whether magnetic susceptibility here is simply a function of grain-size - possibly because magnetite is enriched in the finest grain-size fraction. We compared magnetic susceptibility (Kp)

with percent clay fraction (Ehrmann, this volume) for the zone below 63.2 mbsf. There is no significant correlation ($R = 0.18$). The down-core trend in clay is somewhat similar to that of silt (Ehrmann, pers. comm.), so there is probably no correlation of magnetic susceptibility with any grain-size fraction, because weight % of fraction >63 μm would be a mirror image of clay plus silt which appears not to correlate with susceptibility. This generalisation is consistent with trends of susceptibility within individual sequences. For example, fining upward within sequence 2 is associated with decrease in magnetic susceptibility, whereas the opposite is observed for fining upward within sequences 3 and 4 (Fig. 7). It is interesting to note that susceptibility is increased in cycles 2, 3, 4 and part of 5 compared to other cycles. This is also observed for most environmental magnetic properties in the same depth intervals, and these changes do not correlate with any other data from the CRP-1 record (Sagnotti et al., this volume). High magnetic mineral concentration can be controlled by environmental conditions such as weathering (Sagnotti et al., 1998). We therefore conclude that magnetic susceptibility below 63.2 mbsf is probably related to sequences, although the causes of fluctuations seem to be complex and are not understood at the present state of the study. The signature is probably related to environmental change or different environmental conditions during the build-up of individual sequences which cannot be described in simple terms of lithology (*e.g.*, lonestone abundance or grain-size).

(ii) What causes the rapid two-step increase of magnetic susceptibility above 63.2 mbsf? The interpretation of this change is obvious. The onset of volcanism in the McMurdo Volcanic Province at about 19 Ma (Kyle, 1990) resulted in a strong increase in the input of lava fragments and volcanic clasts, observed above about 62 mbsf and about 33 mbsf in the CRP-1 core (Cape Roberts Science Team, 1998). The semi-quantitative record of volcanic particle abundance, classifying them as common (5-20%) or abundant (>20%), is highly consistent with the pattern of magnetic susceptibility in the upper part of the core. We conclude that an increased input of magnetic particles derived from the volcanic activity of the McMurdo Volcanic Province controls magnetic susceptibility above 62.3 mbsf. This additional input of magnetic grains probably dominates background input of magnetites from other sources, masking both any correlation of magnetic susceptibility to sequences and a possible shift at the Quaternary/Miocene unconformity (43.15 mbsf).

MAGNETIC SUSCEPTIBILITY - INDICATOR OF HIGH-FREQUENCY OSCILLATIONS?

On a depth scale of 150 m it appears that some scatter is superimposed on the large-scale trends of magnetic susceptibility in CRP-1 (Fig. 7). Can these fluctuations be described as cycles with a much higher frequency than those described above? We compare and discuss three sections of the Miocene record where high frequency fluctuations are observed (Fig. 8) and in which the lonestone volumes are near-zero (Brink et al., this volume).

The first example is from Unit 5.1 - just underneath the unconformity between Quaternary and Miocene (Fig. 8a). The fluctuations of magnetic susceptibility appear more as distinct spikes well above the background level rather than cyclic oscillations. Also, the lithological change from sandstone to sandy mudstone is gradual rather than abrupt. This is consistent with the general observation that susceptibility is not primarily controlled by lithology. We interpret this pattern as typical of the entire upper part of the core above 63.2 mbsf. Spikes are probably caused by layers more enriched in magnetic grains derived from the McMurdo Volcanic Province as discussed above. This pattern implies that the input from volcanic sources is discrete rather than randomly distributed over larger core intervals. Possibly, magnetic susceptibility may be useful to detect single volcanic events in the record.

The second example is from Unit 6.2, a medium-bedded fine to coarse sandstone, weak to moderately bioturbated and poorly to moderately sorted. The sandstone is intercalated with clayey siltstone (Fig. 8b). The pattern is similar to that above: characterised by distinct spikes rather than cyclic oscillation. Also, boundaries in lithology are not strictly indicated by susceptibility although sandstone appears to have spikes of higher amplitude than siltstones. There is no obvious explanation for these spikes at present because Unit 6.2 is deposited prior to the onset of the McMurdo volcanic activity.

The third example is from the lowermost Unit 7.1, the only claystone unit of the CRP-1 core (Fig. 8c). Here, magnetic susceptibility oscillations are much more regular than in the other examples above. One spike at about 144 mbsf can be explained by a larger clast visible in the core (Cape Roberts Science Team, 1998). Variation in grain size from mudstone dominated to siltstone dominated at about 146 mbsf does not appear to change the pattern. The observed cyclicity is similar to oscillations in high-resolution physical property records which were explained by Milankovitch forcing (*e.g.*, Bloemendal & de Menocal, 1989; Mienert & Chi, 1995) and often used for time-scale tuning (Shackleton *et al.*, 1995). Unit 7.1 appears to be characterised by much lower sedimentation rates than all other overlying units, and it comprises facies indicative of higher sea level and more distal conditions with respect to the ice margin (Cape Roberts Science Team, 1998). From the preliminary chronology of the CRP-1 record (Cape Roberts Science Team, 1998), the time recorded in the siltstone and mudstone dominated part of Unit 7.1 is estimated to be about 2.1 Ma. The 22 susceptibility cycles evident in this record (Fig. 8c) are consistent with a 100 k.y. eccentricity cycle. On the other hand, the preliminary magnetostratigraphy of plug samples taken at 30-cm spacing alternated between normal and reversed polarity (Cape Roberts Science Team, 1998). Subsequent sampling and analysis revealed even more apparent polarity reversals in Unit 7.1, closely following the fluctuations in magnetic susceptibility, which makes it difficult to interpret the reversal record in terms of the magnetic polarity time scale (Roberts *et al.*, this volume). Alternative interpretations of the magnetic susceptibility record should therefore be tested, including high resolution variability of grain-size

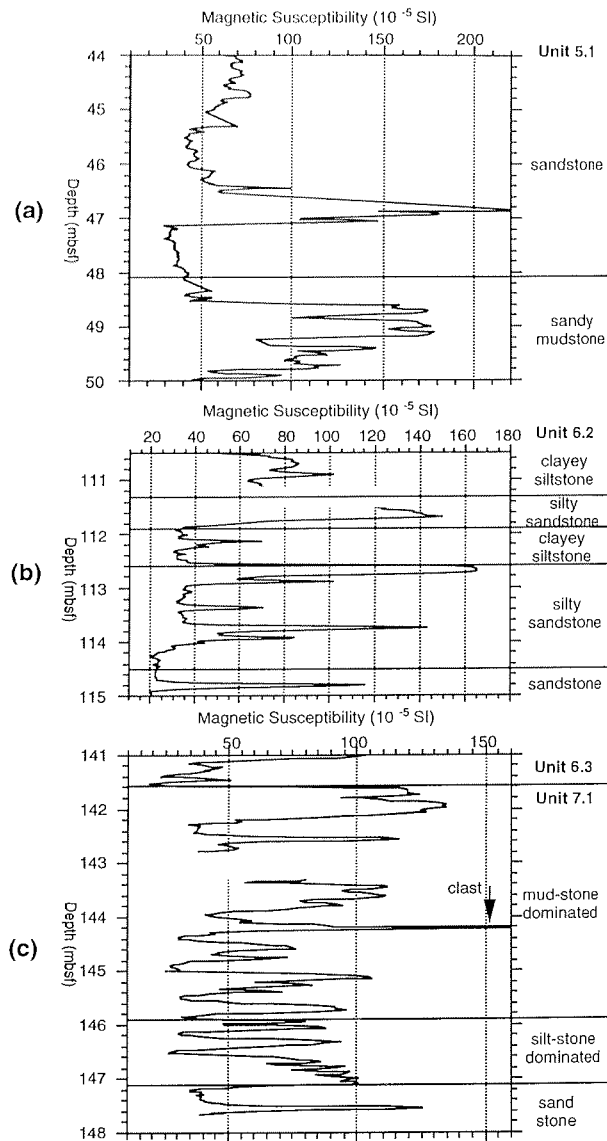


Fig. 8 - Details from the magnetic susceptibility log (K) of figure 6, for: (a) Unit 5.1, (b) Unit 6.2, and (c) Unit 6.3.

by intercalation with distal turbidites (Howe *et al.*, this volume) or artifacts from the drilling operation. At present, grain-size data (De Santis & Barrett, this volume; Woolfe *et al.*, this volume) have insufficient resolution for a detailed comparison with the magnetic susceptibility record. We conclude that the cause of the distinct magnetic susceptibility fluctuations in Unit 7.1 remains uncertain. The hope is that CRP-2 will duplicate the section and, by drilling deeper, will also improve chronological control for the lower part of the CRP-1 section.

CLUSTER ANALYSIS OF DOWNCORE VARIATIONS IN PHYSICAL PROPERTIES - IMPLICATIONS FOR STRATIGRAPHY

A cluster analysis combining the physical properties V_p , WBD, and logarithm of magnetic susceptibility (logsus) revealed five clusters of which the characteristics are summarised in figure 9. In addition to the three

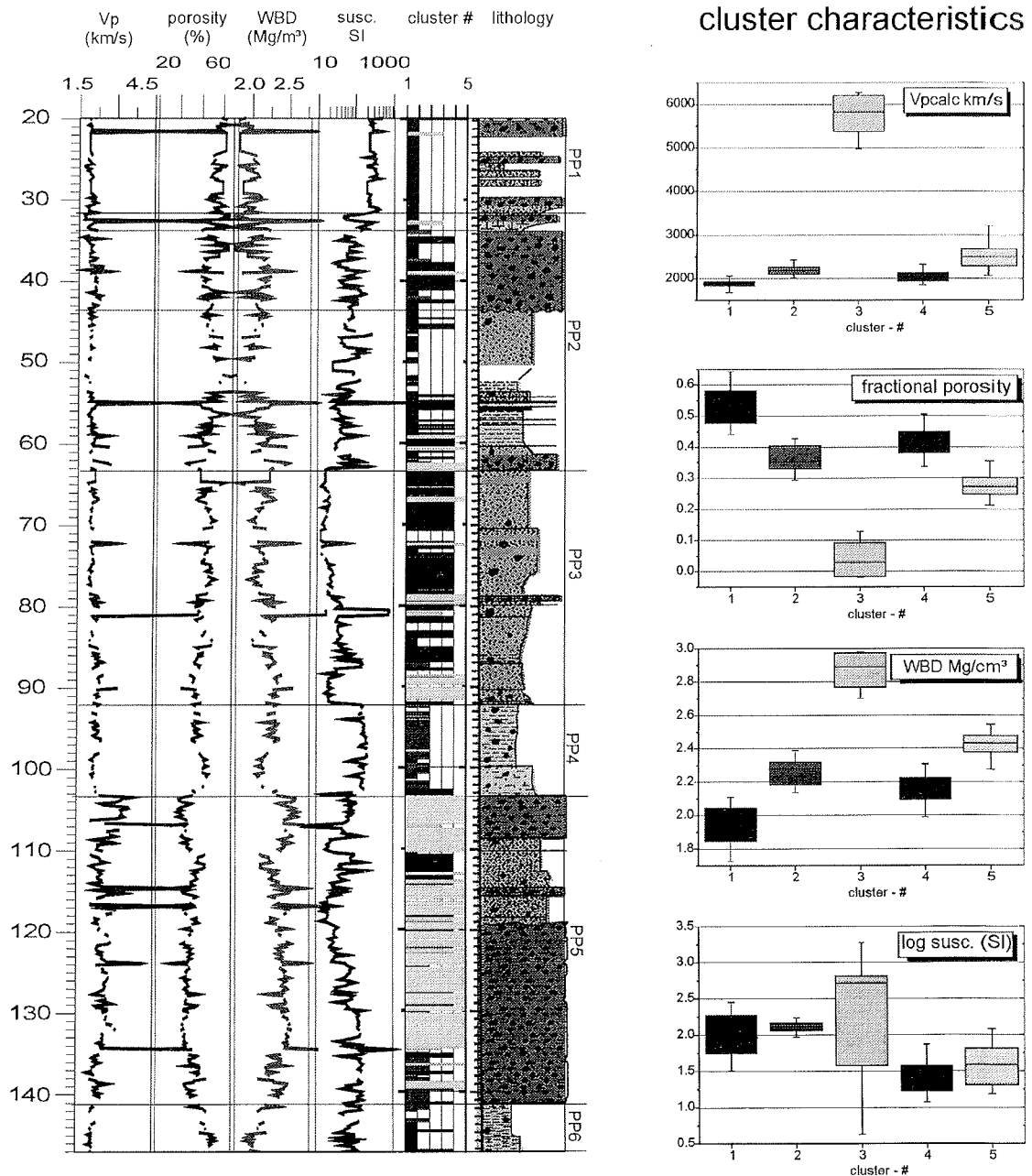


Fig. 9 - Results of a cluster analysis performed on resampled (10-cm depth interval) logs of velocity, WBD (Fig. 2), and magnetic susceptibility (Fig. 6). The continuous velocity record is based on merging core measurements (core logger) with calculations from WBD where velocity data are not available (for further details see "Methods").

parameters used for calculation, porosity and cluster characteristics are shown in the logs (Fig. 9). A plot of cluster *versus* depth shows four major features:

- 1 - there is a lot more downcore variation in clusters than there are lithological units. If each cluster change with depth would define the boundary of a cluster unit, more than 100 such units would result, whereas there are only 18 main lithological units defined in the Initial Report (Fig. 9). Probably the relatively high degree of dispersion and high resolution fluctuations (see above) in the physical property data lead to frequent fluctuations in the cluster record;
- 2 - there is a predominance of some clusters in different depth sections of the core which suggests that a

simplification based on cluster pattern can be carried out. For example, cluster 1 dominates the upper part of the core down to about 63 mbsf. This is followed by a section with predominance of cluster 4 and 5 to 92 mbsf. Cluster 2 is prominent in the underlying unit down to 103 mbsf. Most of the lower part of the core, between 103.41 and about 134 mbsf, is characterised by cluster 5; an exception is the section 110-114 mbsf, which is cluster 4. From 134 mbsf to the base of the core is a generally gradual decrease from cluster 5 to cluster 1;

- 3 - cluster boundaries and cluster patterns are partly consistent but mostly inconsistent with the lithological boundaries (Fig. 9). In addition there is some consistency, but also inconsistency, with the six

physical property (PP) units defined in the Initial Report (Fig. 9). Consistency is almost perfect between 90 and 105 mbsf for the change from cluster 5 to 2 and back to 5 at the boundaries between lithological Units 5.7 to 5.8 and 6.1 to 6.2, respectively, which also define the physical property unit boundaries of PP4. Most other boundaries of the PP and lithological units do not match exactly;

- 4 - cluster 3 is only represented by a few very thin intervals in the entire core. The very high Vp and WBD, very low porosity, and relatively large logsus range (Fig. 9) indicate that this cluster consists mainly or entirely of clasts of various provenance.

Whenever cluster boundaries match PP and lithological units, no additional information is gained. For these sediment sections the use of cluster analysis need not be discussed in detail. In contrast, why can statistically calculated clusters define different boundaries than optically determined physical property and lithological units?

One simple reason is that cluster analysis is objective, whereas the other method is subjective. There are two examples in the record for which this is apparent. Unit PP1 was defined entirely by magnetic susceptibility values always above 100 (10^{-5} SI), which is an obvious and clear, but subjective decision to match a PP-unit with a lithological boundary. More objectively, the cluster analysis places a boundary slightly deeper in the core because the critical susceptibility level to define a cluster is placed at about 1.75 (log susceptibility, Fig. 9), which is lower than 100 (10^{-5} SI). In addition, cluster determination was affected by WBD and Vp which do not change much at the PP1-PP2 boundary; but do change significantly slightly deeper in the core (Fig. 9). Another example is seen near the bottom of the core. The lithological boundary between Units 6.3 and 7.1 is sharp in the lithology log but gradational in both the changes of cluster and the porosity log. The upper PP6 boundary was defined by porosity above 0.4 which was subjectively placed into the centre of the gradient to be consistent with the boundary of the lithological log.

The implication from the cluster analysis is that, in combination with the lithological logs, gradients in the record become more obvious if boundaries do not match. This could yield important information for palaeo-environmental interpretation. For example, the detected physical property gradient at the unit boundary 6.3 to 7.1 may be explained by changes in the matrix, such as grain size or fabric, which can easily be overlooked or underestimated in a lithological description, in which lonestone content plays an important role. It is interesting to note that lonestone volumes have no significant influence on the physical properties including WBD (or calculated porosity), Vp and magnetic susceptibility except for very few large or highly magnetic lonestones (see above, Niessen & Jarrard, this volume). This is also shown by the cluster analysis because cluster 3, indicating lonestones, is hardly present in the cluster record (Fig. 9). The physical properties may suggest that environmental change from ice-distal to more ice-proximal between the deposition of Units 7.1

and 6.3 is less distinct than indicated by the lithological log and sequence stratigraphic interpretation (Cape Roberts Science Team, 1998; Fielding & Woolfe, this volume). Alternatively, the gradient in the physical properties between Units 6.3 and 7.1 may be caused by a downcore gradient from very strong overconsolidation of Unit 6.3 to less overcompaction of the underlying Unit 7.1 as discussed above. Physical gradients formed after deposition by ice-loading can hardly be seen macroscopically during a lithological description.

In summary, cluster analysis of the physical properties logs shows that these logs do not simply respond to gross stratigraphy and subjectively defined physical property units. Instead, the clusters appear to carry information concerning subtler, as-yet-unidentified petrophysical variations at CRP-1 and to detect inconsistencies with other results which are worth more detailed analysis. Consequently, both lithological unit boundaries and sequence boundaries generally do not match cluster boundaries. More intensive work is necessary to compare the comprehensive results from various disciplines which produced data on the CRP-1 core (this volume), in order to understand the significance of the cluster pattern as shown in figure 9. We do not suggest that meaningful physical property units as defined by the Cape Roberts Science Team (1998) are to be replaced by cluster boundaries. Instead, both subjective and objective methods should be combined to distinguish between sharp and transitional boundaries in order to improve the palaeo-environmental interpretation.

CONCLUSIONS

From the down-core trends of physical property logs and comparisons of physical properties with other data we can draw the following major conclusions for the CRP-1 site:

- 1 - if not simply caused by poor data quality, the lack of a step decrease in porosity at the 43.15 mbsf unconformity between the Quaternary and Miocene sediments, despite exhumation, may be explained by the transition from smectite-rich uppermost Miocene to smectite-poor Quaternary sediments. Smectite can introduce an undetected matrix density change that may obscure a subtle porosity offset;
- 2 - a large part of the Miocene record has been overconsolidated by ice loading, resulting in an enormously steep compaction trend. Overcompaction includes not only diamictites (interpreted as basal till), but also underlying sand, silt and mud units because their compaction is much higher than expected from burial depth and grain size. Overconsolidation is not clearly evident for Quaternary units;
- 3 - based on typical compaction trends of marine sediments, the maximum burial and subsequent exhumation of the Miocene section is estimated to be between 200 and 700 m, depending on whether possible overcompaction of some Miocene units with relatively high porosities is ignored or not;

- 4 - the onset and activity of the McMurdo Volcanic Province at about 19 Ma can be traced using high-resolution magnetic susceptibility. Increased concentrations of volcanic glass and lava fragments above 63.2 and 33 mbsf are consistent with a strong two-step increase in magnetic susceptibility;
- 5 - the downcore pattern of magnetic susceptibility below 63.2 mbsf appears to be related to sequences although the causes remain uncertain. The large-scale susceptibility signature is probably related to environmental change and cannot be described in terms of limestones abundance, grain-size or lithology in general;
- 6 - regular high-frequency oscillations of magnetic susceptibility are only observed in Unit 7.1. They may indicate 100-k.y. eccentricity cycles or may be caused by cyclic intercalation of distal turbidites or artifacts from the drilling operation;
- 7 - cluster analysis of the physical properties logs shows that these logs do not simply respond to gross stratigraphy but carry information concerning subtler, as-yet-unidentified petrophysical variations at CRP-1.

ACKNOWLEDGEMENTS

We are grateful to Antarctica New Zealand and, in particular, the CRP-1 project staff for providing excellent transportation, accommodation and laboratory facilities during the field work. Conrad Kopsch (Alfred Wegener Institute, Potsdam, Germany) is acknowledged for taking care of the technical part of the whole-core measurements and the data acquisition. Without financial support of the Alfred Wegener Institute to the Cape Roberts Project, the participation of F. Niessen in the project would not have been possible. R.D. Jarrard thanks the National Science Foundation for financial support (OPP-9418429). We are grateful to two anonymous referees whose valuable comments improved the quality of this manuscript substantially. This is contribution No. 1485 of the Alfred Wegener Institute for Marine and Polar Research.

REFERENCES

- Bloemendal J. & deMenocal P., 1989. Evidence for a change in the periodicity of tropical climate cycles at 4.4 Myr from whole-core magnetic susceptibility measurements. *Nature*, **342**, 897-900
- Brückmann W., 1989. Typische Kompaktionsabläufe mariner Sedimente und ihre Modifikation in einem rezenten Akkretionskeil (Barbados Ridge). *Tübinger Geowiss. Arbeiten*, **A**, **5**, 1-135.
- Cape Roberts Science Team, 1998. Initial Report on CRP-1, Cape Roberts Project, Antarctica. *Terra Antarctica*, **5**(1), 187 p.
- Davis J.C., 1973. *Statistics and Data Analysis in Geology*. Wiley, New York.
- Foscolos A.E., 1990. Catagenesis of argillaceous sedimentary rocks. In: McIlreath I.A. & Morrow D.W. (eds.), *Diagenesis*, Runge Press Ltd., Ottawa, 177-187.
- Hamilton E.L., 1976. Variations of density and porosity with depth in deep-sea sediments. *J. Sediment. Petrol.*, **46**, 280-300.
- Hamilton E.L., 1979. Sound velocity gradients in marine sediments. *J. Acoust. Soc. Am.*, **65**, 909-922.
- Hayes J.B., 1979. Sandstone diagenesis - the hole truth. In: Scholle P.A. & Schluger P.R. (eds.), *Aspects of Diagenesis, SEPM Special Publ.*, **26**, 127-139.
- Heasler H.P. & Kharitonova N.A., 1996. Analysis of sonic well logs applied to erosion estimates in the Bighorn Basin, Wyoming. *AAPG Bull.*, **80**, 630-646.
- Hedberg H.D., 1936. Gravitational compaction of clays and shales. *Am. J. Sci.*, **5**(31), 241-287.
- Hutcheon I., 1990. Aspects of the diagenesis of coarse-grained siliciclastic rocks. In: McIlreath I.A. & Morrow D.W. (eds.), *Diagenesis*, Runge Press Ltd., Ottawa, 165-176.
- Kyle P.R., 1990. McMurdo Volcanic Group, western Ross embayment. In: LeMasurier W.E. & Thomson J.W. (eds.), *Volcanoes of the Antarctic Plate and Southern Oceans, AGU, Antarctic Research Series*, **48**, 19-25.
- Magara K., 1980. Comparison of porosity-depth relationships of shale and sandstone. *J. Petroleum Geol.*, **3**, 175-185.
- Mienert J. & Chi J., 1995. Astronomical time-scale for physical property records from Quaternary sediments of the northern North Atlantic. *Geol. Rundsch.*, **84**(1), 67-88.
- Ollier G. & Mathis B., 1991. Lithologic interpretation from geophysical logs in Holes 737B, 739C, and 742A. *Proc. ODP, Sci. Results*, **119**, 263-289.
- Sagnotti L., Florindo F., Verosub K.L., Wilson G.S. & Roberts A.P., 1998. Environmental magnetic record of Antarctic palaeoclimate from Eocene/Oligocene glaciomarine sediments, Victoria Land Basin. *Geophysical Journal International*, **134**, 653-662.
- Serra O., 1986. *Fundamentals of Well Log Interpretations: The interpretation of logging data*. Amsterdam, Elsevier.
- Shackleton N.J., Crowhurst S., Hagelberg T., Pisias N.G. & Schneider D.A., 1995. A New Late Neogene time scale: application to Leg 138 sites. *Proc. ODP, Sci. Results*, **138**, 73-101.
- Shumway G., 1960a. Sound speed and absorption studies of marine sediments by a resonance method, Part 1. *Geophysics*, **25**, 451-467.
- Shumway G., 1960b. Sound speed and absorption studies of marine sediments by a resonance method, Part 2. *Geophysics*, **25**, 659-682.
- Taylor J.M., 1950. Pore space reduction in sandstones. *AAPG Bull.*, **23**, 701-717.
- Thompson R. & Oldfield F., 1986. *Environmental Magnetism*. Allen & Unwin, London, 227 p.
- Weber E.M., Niessen F., Kuhn G. & Wiedicke M., 1997. Calibration and application of marine sedimentary physical properties using a multi-sensor core logger. *Marine Geology*, **136**, 151-172.
- White P., 1989. Downhole Logging. In: Barrett P.J. (ed.), *Antarctic Cenozoic history from the CIROS-1 drillhole, McMurdo Sound, DSIR Bulletin*, **245**, 7-14.